Talanta 81 (2010) 424–432

Contents lists available at ScienceDirect

Talanta

journal homepage: www.elsevier.com/locate/talanta

Adsorption of divalent heavy metal ions onto IDA-chelating resins: Simulation of physicochemical structures and elucidation of interaction mechanisms

Panpan Ling[a], Fuqiang Liu[a,b,*], Lanjuan Li[a], Xiaosheng Jing[a,c], Baorui Yin[a], Kaibo Chen[a], Aimin Li[a,b]

[a] State Key Laboratory of Pollution Control and Resource Reuse, School of the Environment, Nanjing University, Nanjing 210093, PR China
[b] State Environmental Protection Engineering Center for Organic Chemical Industrial Waste Water Disposal Resource Reuse, Nanjing 210046, PR China
[c] Shaanxi Institute for Environmental Science Research and Design, Shaanxi 710054, PR China

ARTICLE INFO

Article history:
Received 20 August 2009
Received in revised form
10 December 2009
Accepted 13 December 2009
Available online 21 December 2009

Keywords:
Chelating resin
Heavy metal ion
Iminodiacetic acid group
Physicochemical structure
Adsorption mechanism

ABSTRACT

The adsorption performances, under static as well as dynamic conditions, for such metal ions as Cu(II), Pb(II) and Cd(II) toward chelating resins (IRC748 and NDC702) similarly containing iminodiacetic acid group but diverse pore structures, are systematically performed and deeply exploited. The physicochemical characteristics of both IDA-chelating resins are thoroughly explored by EA, FT-IR, SEM-EDX and PSD. Langmuir isotherm and pseudo-second-order equation could satisfactorily describe the batch experimental data, based on which the equilibrium and kinetic parameters are calculated and compared. The adsorption capacities follow the order of Cu(II) > Pb(II) > Cd(II), due to the complicated impacts of metal ion electronegativity as well as resin pore textures. In the contrast of single and binary adsorption performances, more reduction of Cd(II) than Cu(II) is expectably investigated with the coexistence of competitive ion since the less affinity and hence weak competition of the former onto solid-phase. Using aqueous solution of 15 wt% HCl, nearly 100% recovery of Cu(II) and Cd(II) from IDA-resins could be strictly achieved in the column-tests. Furthermore, a schematic illustration of possible pore structure has been proposed and simulated. Meanwhile, the interaction mechanisms are thereby deduced and evidently confirmed by FT-IR as well as SEM analysis.

1. Introduction

Major sources of heavy metal release to the environment include metal extraction, tannery, petroleum refining, metal fabrication and surface finishing, paints, pigment as well as the battery manufacturing industries [1,2]. Such heavy metal ions as copper, lead, and cadmium, dis-biodegradable, high-toxic and susceptible-carcinogenic, impose harmful effects on proteins, enzymes and human-life [1,3]. Hence, water contamination with heavy metals has caused comprehensive and increasing concerns from a healthy point of view [3–5]. Many methods, including precipitation, electrodeposition, electrocoagulation, membrane separation, ion-exchange and adsorption, have been developed to remove heavy metals from waste-streams [6–10]. The main shortcoming exists in the large consumption of chemicals, which implies relatively higher operating cost as well as voluminous sludge production [1]. In addition, the above-mentioned technologies are nearly nonselective, thus caused much difficulty in fulfilling drainage standard at a low-down level and putting multi-metal mixtures into satisfactory application. For the purpose of removing and reusing metals with much efficiency and high selectivity, both synthesis of new materials and improvement of traditional techniques have tend to be accredited. For instance, new materials involving polymeric cation exchanger [11,12], carbon nanotubes [13,14], organically modified clay [15], amino-modified or pore-expanded mesoporous silica [16,17], nitrogen- and oxygen-decorated carbon [14,18], nano-iron [19], activated red mud [20], offer high capacities or fast kinetics toward metal ions even in the presence of competing ions or at a high salinity. Among these materials, ion exchanger is highly popular and widely applied recently, whose major development trends to abundantly functional chelators. As is well-known to all, chelating resins with various ligands could selectively bond with certain metal cations and thus own a foreground since their integrated interactions involving ion-exchange, physic-sorption and chelation [12,21,22]. Based on the provision of electron pairs and the formation of stable covalent complexes with bivalent metals, chelating resins containing iminodiacetic acid (IDA), for instance, the commercial products from Rohm & Haas (Amberlite IRC748), Purolite (S930), Bayer (Lewatit TP207) or tentatively synthesized by researchers themselves (Chelex-100 in Bio-Rad Laboratories, Richmond), are prior to be investigated solely, focusing on the effects of temperature, pH-value, time and ion-strength upon adsorp-

* Corresponding author at: State Key Laboratory of Pollution Control and Resource Reuse, School of the Environment, Nanjing University, 22 Hankou Road, Nanjing 210093, Jiangsu Province, PR China. Tel.: +86 25 86087695; fax: +86 25 85572627.
E-mail address: jogia@163.com (F. Liu).

0039-9140/$ – see front matter © 2009 Elsevier B.V. All rights reserved.
doi:10.1016/j.talanta.2009.12.019

tion equilibrium, thermodynamics, kinetics, dynamics, competitive selectivity and regeneration [10,23–26].

Among the important factors possibly influencing the removal of solute from aqueous media, the role of pore structure and pore size distribution in relation to the size of the contaminant molecule, which is invaluable in the selection of a novel adsorbent or the application in an effective manner especially as to some organic pollutants, however, has seldom been exploited according to heavy metal ions [27]. Both ligand-type and pore-structure of adsorbents are proved crucial in adsorption processes. For example, as for a novel hybrid membrane, the large surface area, high ligand density and suitable interconnected 3D hierarchical porous surface have been testified the main cause of remarkably high copper ion binding capacity [28]. In other instances, coconut shell or coal derived carbons as well as polymer-impregnated carbon have exhibited enhanced heavy metal ion uptake, which might contribute to their high surface area and facile mass diffusion [29,30]. Otherwise, the adsorption capacities of chemically pretreated ACF for copper and cadmium are augmented with the increase in the oxygenous groups and the number of micropores [31]. Consequently, not only the functional groups but also the pore characteristics of adsorbents are of much importance in the affinities towards both organic and inorganic pollutants.

In the present work, the commercial IDA-chelating resin IRC748 and lab-simulated product NDC702 with similar functional groups but diverse pore structures, were selected as the novel adsorbents. The adsorption performances for such divalent heavy metal ions as Cu(II), Pb(II) and Cd(II), involving equilibrium, kinetics, dynamics and binary competition, were thoroughly compared and systematically evaluated, based on which the interaction mechanisms were herewith rationally deduced and briefly illuminated. Furthermore, the physicochemical structures were roughly simulated and morphologically depicted.

2. Experimental

2.1. Materials

Amberlite IRC748 (Rohm & Haas Co.) was macroporous styrene divinylbenzene chelating resins with an iminodiacetic acid functional group.

The lab-simulated product NDC702 was synthesized as follows (Scheme 1):

1. About 80 g of the chloromethylated styrene divinylbenzene copolymer beads (provided kindly by Jinxiang Chemical, PR China. Cross-linking density about 8% and the chloral content about 17%) mixed with excess hexamethylene tetramine and ethanol, was stirred at 323 K for 18 h to obtain polybenzylamine.
2. 50 g above-mentioned cross-linking polybenzylamine was mixed with 600 mL 6% chloroacetic acid solution, then the pH 9 was adjusted by sodium hydroxide, and the mixture was stirred continuously at 333 K for 10 h, then 353 K for 2 h.

Prior to use, both adsorbents were extracted by ethanol for 6 h followed by washing with 1 M NaOH, distilled water, 1 M HCl, distilled water until neutrality. The H-form resins were then dried at 333 K and the fraction 30–50 mesh was collected and used in this work.

Copper nitrate, lead nitrate, and cadmium nitrate were analytical reagents purchased from Nanjing NingShi reagent company.

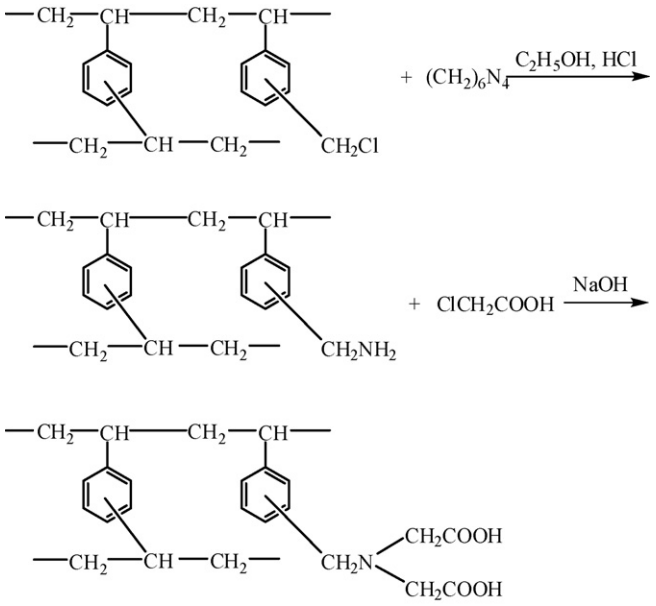

Scheme 1. The synthesis of lab-simulated product NDC702.

2.2. Characterization of IDA resins

The functional groups of NDC702 and IRC748 were analyzed by Fourier transform infrared spectroscopy (FT-IR, Nicolet 170 SX) and element analysis (EA, Elementar Vario MICRO). The surface area and pore size distribution (PSD, ASAP 2020 M + C) were detected by adsorption of nitrogen using the BET equation. The surface and section morphologies and elements of polymer beads were examined with a scanning electron microscope-energy dispersive X-ray spectroscopy (SEM-EDX, S-3400N II).

2.3. Adsorption/desorption experiments

2.3.1. Single adsorption isotherms

Adsorption of Cu(II), Pb(II) and Cd(II) ions from aqueous solutions were studied in batch systems. The initial pH of the sample solutions were adjusted in the range of 1–6 by using dilute solution of HNO_3 or NaOH. All pH measurements were performed with a PHS-3C digital pH meter.

Adsorption isotherms were carried out at an optimum pH-value with different initial concentrations varying from 0.5 to 5 mmol/L of metal while holding the resin amount at a constant value at different temperatures (283, 303, 323 K). The stirring speed was 120 rpm and continued for 24 h. The residual concentrations of the metal ions in solutions were measured by using a flame atomic absorption spectrophotometer (AAS, TAS-990, Beijing Pgeneral Co.). The quantities of metal ions adsorbed per unit mass of the resin were calculated by using the following expression.

$$Q_e = \frac{(C_0 - C_e) \times V}{W} \quad (1)$$

Here, Q_e is the equilibration adsorption capacity of metal ions (mmol/g), C_0 and C_e are the concentrations of the metal ions in the aqueous phase before and after the equilibration, respectively (mmol/L), V is the volume of the aqueous phase (L), and W is the amount of the resin used (g).

The Langmuir and Freundlich isotherm models are employed in this work.

Langmuir equation:

$$\frac{C_e}{Q_e} = \frac{C_e}{Q_0} + \frac{1}{Q_0 b} \quad (2)$$

where C_e is the equilibrium concentration (mmol/L), Q_e the amount of adsorbed material at equilibrium (mmol/g), b the "affinity" parameter or Langmuir sorption constant (L/mmol), which reflects the free energy of sorption, and C_0 the "capacity" parameter (mmol/g) [19,20].

The empirical Freundlich equation:

$$Q_e = K_f C_e^{1/n} \quad (3)$$

where Q_e is the equilibrium capacity (mmol/g), C_e the equilibrium concentration (mmol/L), K_f and n the constant isotherm parameters [19,20].

2.3.2. Single and binary kinetics

The rate of loading of metal ions on the resins was determined under the following conditions: 1000 mL metal ion solution (1 mmol/L) was stirred with 1.00 g resin at 303 K. An aliquot of 1 mL solution was removed at predetermined intervals for analysis by AAS and the amount of metal ions loaded on the resin phase was calculated.

The pseudo-first-order kinetic model is given as:

$$\log(Q_e - Q_t) = \log Q_e - \frac{k_1 t}{2.303} \quad (4)$$

The pseudo-second-order equation may be expressed as:

$$\frac{t}{Q_t} = \frac{1}{(k_2 Q_e^2)} + \frac{t}{Q_e} \quad (5)$$

The intraparticle diffusion rate can be described as:

$$Q_t = k_{\text{int}} t^{1/2} \quad (6)$$

where Q_t is the adsorption capacity in time t (mmol/g), Q_e the adsorption capacity at equilibrium (mmol/g) and k_1, k_2, k_{int} is the adsorption rate constant of pseudo-first-order (min^{-1}), pseudo-second-order (g/mmol/min), intraparticle diffusion rate ($\text{mmol/g/min}^{1/2}$), respectively [32].

2.3.3. Single and binary dynamics

About 2.4 mL resin was placed in a glass column (the length of 240 mm and the diameter of 10 mm). Solution of metal ions with initial concentration of 5 mmol/L was allowed to flow gradually through the column at rate of 10 BV/h (Bed Volume per hour) and 303 K. The stripping of the metal was carried out with 15 wt% HCl at 2.5 BV/h.

3. Results and discussion

3.1. Characterization of IDA-chelating resins

3.1.1. Chemical structure

3.1.1.1. Elemental analysis. The results of the elemental analysis of C, H, N, O of the resins were given in Table 1. The content of nitrogen and oxygen for NDC702 and IRC748 was 5.00% and 5.74%, 20.58% and 21.22%, respectively. Higher nitrogen and oxygen content was observed in the case of IRC748.

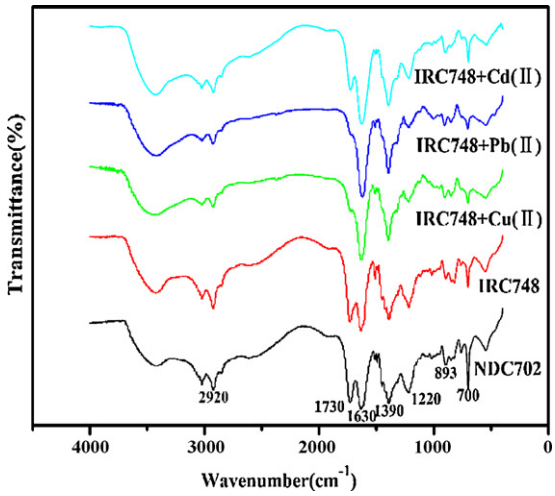

Fig. 1. FT-IR spectra of NDC702, IRC748 before and after adsorption.

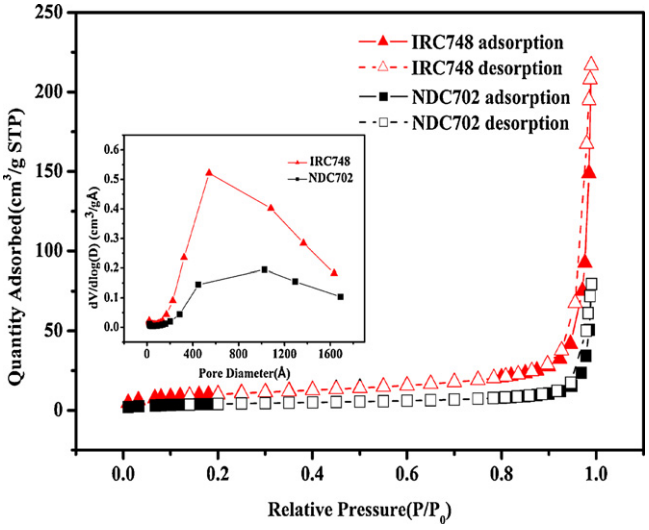

Fig. 2. N_2 sorption/desorption isotherms and PSD curves of NDC702 and IRC748.

3.1.1.2. FT-IR spectra. The FT-IR spectra of both resins were presented in Fig. 1. The absorption band near 1730, 1220 cm^{-1} was caused by the stretching vibrations of the carbonyl groups. The absorption feature near 1390 cm^{-1} corresponds to OH bending, indicating the presence of protonated carboxylic groups. The stretch absorptions of carboxylic hydroxyl groups occurred between 2500 and 3400 cm^{-1}. A band of intensity at about 1100 cm^{-1} is conspicuously absent, indicating that the nitrogen atom in the imino group is still protonated at the working pH [33,34]. EA and FT-IR spectrum showed both IDA-chelating resins tested were chemically similar.

3.1.2. Physical structure

3.1.2.1. Adsorption isotherms of nitrogen. Fig. 2 shows the adsorption–desorption isotherms of nitrogen at 77 K on both

Table 1
Some typical physicochemical characteristics of the resins IRC748 and NDC702.

Sample	Element content (%)				S_{BET} (m^2/g)	V_t (cm^3/g)	V_{mi} (cm^3/g)	Pore size (nm)
	C	H	N	O				
IRC748	65.40	6.81	5.74	21.22	36.3985	0.3367	0.0044	36.85
NDC702	65.73	6.38	5.00	20.58	14.2367	0.1235	0.0034	34.53

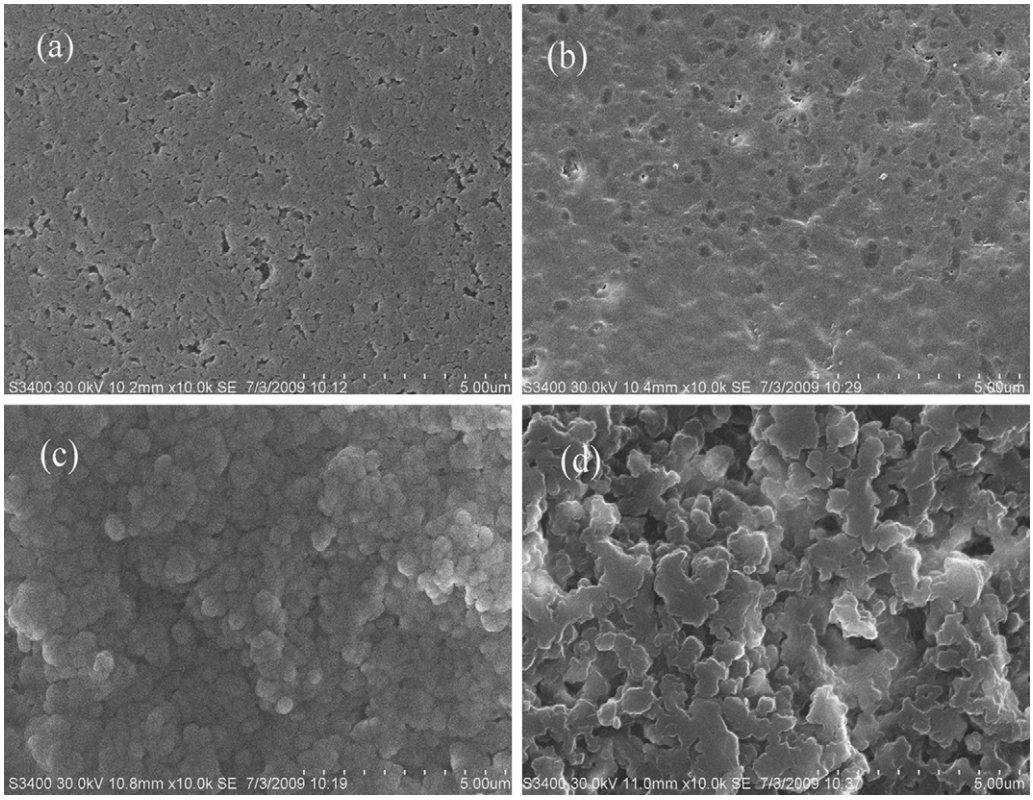

Fig. 3. SEM images of the surface (a and b) and section (c and d) morphologies for IRC748 (a and c) and NDC702 (b and d).

resins. All isotherms exhibit a Type IV profile according to the IUPAC classification with remarkable hysteresis loops in relative pressure higher than 0.9. This implies that the pores comprising the resin specimens are mostly mesoporous and macroporous. Micropore volume is extremely small seen from Table 1, which is preferred from the metal ion adsorption point of view. The hysteresis loops of IRC748 took after the type H3 loop, which is characteristic of the mesoporous materials being comprised of agglomerated pores with broad PSD and indicates an open pore structure [35,36].

PSD curves using BJH method indicated that the amount of mesopores in IRC748 was more than NDC702, which was consistent with data given in Table 1. Further conclusion drawn from SEM images was that the mesopores in IRC748 mainly distributed on surface, which would be discussed later.

3.1.2.2. SEM images. The SEM images in Fig. 3 show the significant morphological differences of the surfaces and sections of both resin beads. The dark spots observed in SEM image of both resins (Fig. 3), may represent the pore openings and cavities. This open structure facilitates solution flow in pores of resins which in turn gives good adsorption kinetics that will be validated in the following experiments. The surface of IRC748 was rough and numerous pores existed (dark spots). In the section image of IRC748, there were few pores or cavities with matrix highly stacked. Reversely, the surface of NDC702 contained lots of fovea and a few slits with abundant pores in section.

3.2. Metal ions adsorption performance

3.2.1. Effect of pH

Solution pH had a strong effect on the adsorption capacity of metal ions (Fig. 4). The adsorption capacity increased as pH value until it reached the highest point near pH 5. This increase was ratio-

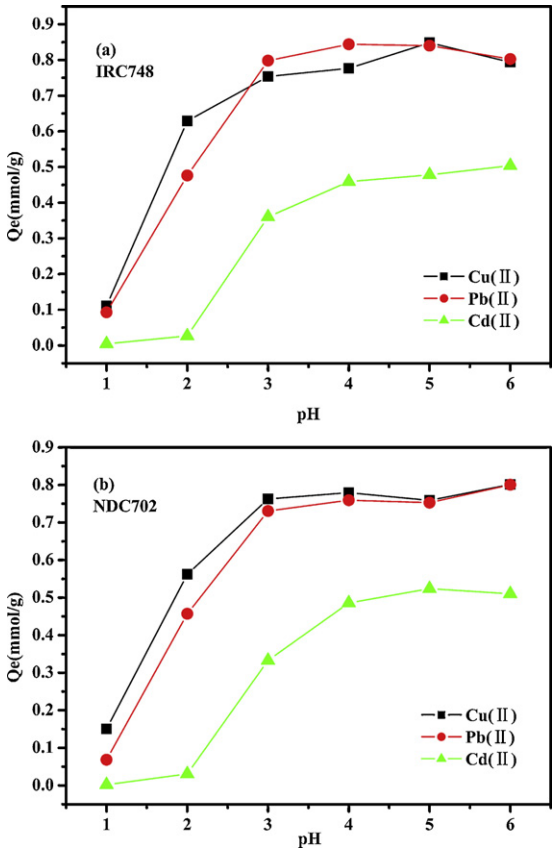

Fig. 4. The equilibrium capacity for Cu(II), Pb(II) and Cd(II) on IRC748 (a) and NDC702 (b) as a function of pH. The initial conditions are the temperature of 298 K, resin dose of 0.05 g, and the metal solution of 1 mM and 50 mL.

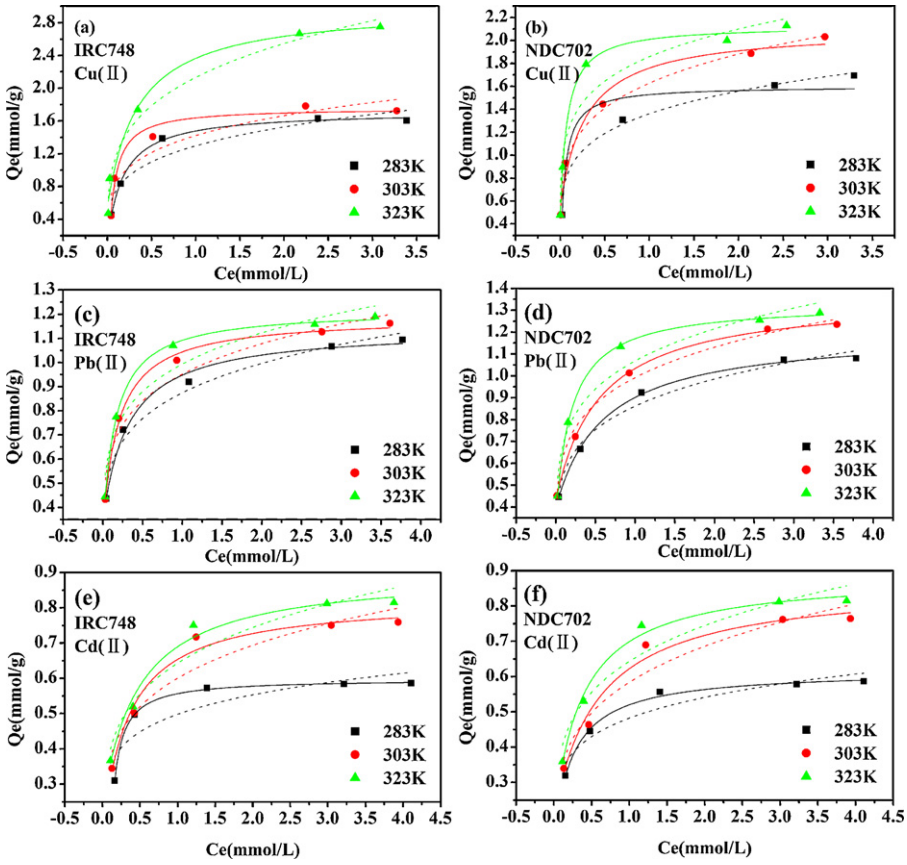

Fig. 5. Comparison of the Langmuir (solid line) and Freundlich (dash line) model fit toward copper (a and b), lead (c and d), cadmium (e and f) onto NDC702 and IRC748.

nal: the IDA group was weakly acidic so that the carboxyl groups on resins were not easily dissociated at lower pH value and there was competitive adsorption between metal ions and hydrogen ions for the binding sites on the surface of the resins. Besides, the whole resin cannot effectively interact with the metal ions due to the protonation of amino groups and the loss of negative charge [37,38]. At higher pH values, the presence of OH^- ions formed the hydroxyl complexes of metal ions which also affected resin capacity. Hence, the following experiments were performed in the solution pH 5 considering easier comparison.

3.2.2. Adsorption isotherms

Equilibrium isotherm, the relation between the amount capacity (Q_e) and the residual concentration in the aqueous phase (C_e), is important to describe how solutes interact with the resins and so is critical in optimizing the use of the resins. Metal ions adsorption isotherms of NDC702 and IRC748 resins are presented in Fig. 5. The amount of three metal ions adsorbed per unit mass of both resins increased with the initial metal concentration and temperature as expected. In this figure, the monolayer Langmuir and empirical Freundlich isotherms are employed to represent the isotherm data. It is apparent that the Langmuir isotherm describes the observed data much better than the Freundlich alternative. The isotherm parameters for copper, lead, and cadmium are listed in Table 2.

It can be seen from Fig. 5 and Table 2 that the maximum uptake on IRC748 and NDC702 follow the same order of Cu(II) > Pb(II) > Cd(II) as metal electronegativity of Cu(1.8) > Pb(1.6) > Cd(1.5) [39]. At the pH-range under this investigation, the surface of the resins is predominantly negative, thus, the Coulombic forces favor the interaction between bivalent cation species and adsorption sites.

As seen from Fig. 5 and Table 2, the uptake of the same metal ion on IRC748 was a little lower than that on NDC702, which attributed to fewer macropores inside the beads of IRC748. That will be further discussed in Section 3.3.

3.2.3. Adsorption kinetics

3.2.3.1. For single system. The pseudo-first-order, pseudo-second-order and intraparticle diffusion models are all applied to interpret the adsorption kinetics. From Table 3, the pseudo-second-order

Table 2
Constant parameters of the Langmuir and Freundlich isotherms.

Resins	Metals	T (K)	Langmuir constants			Freundlich constants		
			Q_0	b	r^2	K_f	n	r^2
IRC748	Cu(II)	283	1.69	7.49	0.999	1.29	3.45	0.917
		303	1.81	9.21	0.998	1.42	3.58	0.858
		323	2.82	9.58	0.997	2.15	3.47	0.963
	Pb(II)	283	1.13	6.91	0.998	0.87	4.90	0.973
		303	1.18	9.52	0.999	0.95	4.93	0.953
		323	1.21	11.64	0.999	1.00	4.98	0.944
	Cd(II)	283	0.61	8.93	0.999	0.49	5.65	0.793
		303	0.80	5.82	0.999	0.60	4.29	0.936
		323	0.86	5.25	0.999	0.64	4.35	0.959
NDC702	Cu(II)	283	1.72	9.53	0.997	1.36	4.57	0.901
		303	2.04	12.66	0.995	1.64	4.44	0.986
		323	2.12	27.75	0.998	1.88	4.93	0.968
	Pb(II)	283	1.12	6.38	0.998	0.86	5.05	0.991
		303	1.28	7.50	0.997	0.99	5.38	0.992
		323	1.31	11.06	0.999	1.07	4.78	0.963
	Cd(II)	283	0.61	6.66	0.999	0.48	5.49	0.929
		303	0.82	3.92	0.998	0.59	3.94	0.916
		323	0.86	3.17	0.999	0.65	4.20	0.912

Table 3
Adsorption kinetic parameters of IRC748 and NDC702.

Resin	Metal	Pseudo-first-order			Pseudo-second-order				Intraparticle diffusion	
		Q_e	k_1	r^2	Q_e	k_2	h	r^2	k_{int}	r^2
IRC748	Cu(II)	0.91	0.04	0.955	0.99	0.05	0.05	0.990	0.03	0.722
	Pb(II)	0.77	0.03	0.954	0.85	0.05	0.04	0.992	0.03	0.773
	Cd(II)	0.49	0.04	0.970	0.54	0.10	0.03	0.994	0.02	0.691
NDC702	Cu(II)	0.97	0.02	0.982	1.10	0.02	0.02	0.994	0.04	0.847
	Pb(II)	0.70	0.02	0.966	0.80	0.02	0.02	0.993	0.03	0.880
	Cd(II)	0.51	0.02	0.971	0.57	0.05	0.02	0.995	0.02	0.822

kinetic model succeeds in describing the kinetic curves. In another hand, the adsorption rate of metal ions extremely depends on the concentration of ions at the adsorbent surface, as reported in an earlier literature [32].

Comparatively, the initial adsorption rate constants (the value of h) of IRC748 for all metal ions are greater than NDC702 due to more suitable pore structure of the former for transporting the adsorbate onto the adsorption sites. What's more, the adsorption rate constant (the value of k_2) of IRC748 equals around twice that of NDC702, which reinforces the argument that the IRC748 chelators bind metal ions quickly for the same reason.

It is worth mentioning that the adsorption of Cu(II) and Cd(II) on NDC702 is greater than IRC748, with the possible mechanism deeply discussed in Section 3.3. Contrarily, the uptake of Pb(II), with the largest ionic radius of 1.32 Å, show a little greater onto IRC748 than that onto NDC702, and the main reason maybe exist in the more outside pores on the surface of the former.

3.2.3.2. For binary system. Adsorption kinetics of coexisting multi-metal ions onto the resins are also exploited, and the results are presented in Fig. 6. Compared with the single systems, the adsorption capacities of both metals on two resins in the binary systems have been reduced whereas with different extent. In detail, the decrease in copper uptake is much lower than cadmium, viz. 2.8% and 62.5% for IRC748, 14.8% and 65.5% for NDC702, respectively. This may be mainly caused by the direct site competition mechanism. The reduction in capacity of IRC748 is less than NDC702 with a narrow pore size distribution, the similar phenomena ever discussed [40]. Supposing that metals compete to the same active sites, those metals with stronger affinity can replace others with weaker affinity [41]. Therefore, the kinetic data indicate that the adsorption affinity of Cu(II) to IDA-resins is greater than Cd(II), in accordance with the above discussions. According to the equilibrium capacity calculated from pseudo-second-order kinetic model, the separation factors α of Cu/Cd for IRC748 and NDC702 reach about 158.1 and 95.6, respectively, which give an abundant confirmation for the notably competitive phenomena in solid phase.

3.2.4. Column adsorption and desorption

3.2.4.1. Column adsorption. Breakthrough curves at a solution flow rate of 10BV/h are shown in Fig. 7. In single system, the breakthrough points ($C_i/C_0 > 0.9$) of Cd(II) on IRC748 and on NDC702 are 216 and 302 BV, respectively. In binary system, the values on IRC748 and NDC702 decrease to 45 and 42 BV, respectively. The breakthrough time of Cd(II) is more than 21 h due to the direct competition for adsorption sites. At the very start, the effluent concentration of Cd(II) is high probably due to the desorption occurring simultaneously. Obviously, the adsorption capacity of Cd(II) decreases sharply in the presence of Cu(II), which reduced from 1.24 to 0.15 mmol/g for IRC748. On the other hand, the decrease

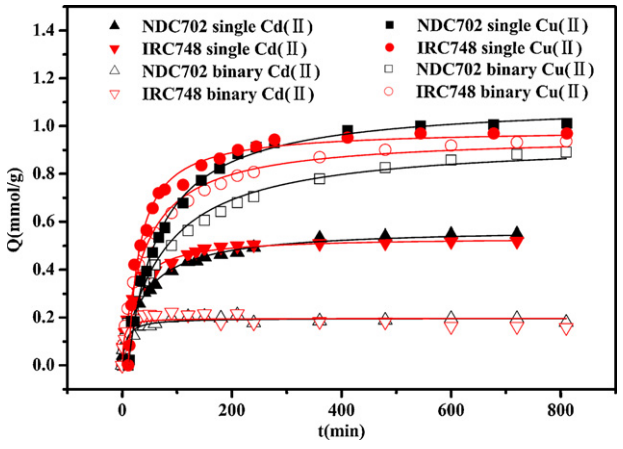

Fig. 6. Effect of the adsorption time on the capacities for Cu(II) and Cd(II) under noncompetitive and competitive conditions at 303 K, 1.00 g resin, pH-value of 5, initial metal ion concentration of 1 mM.

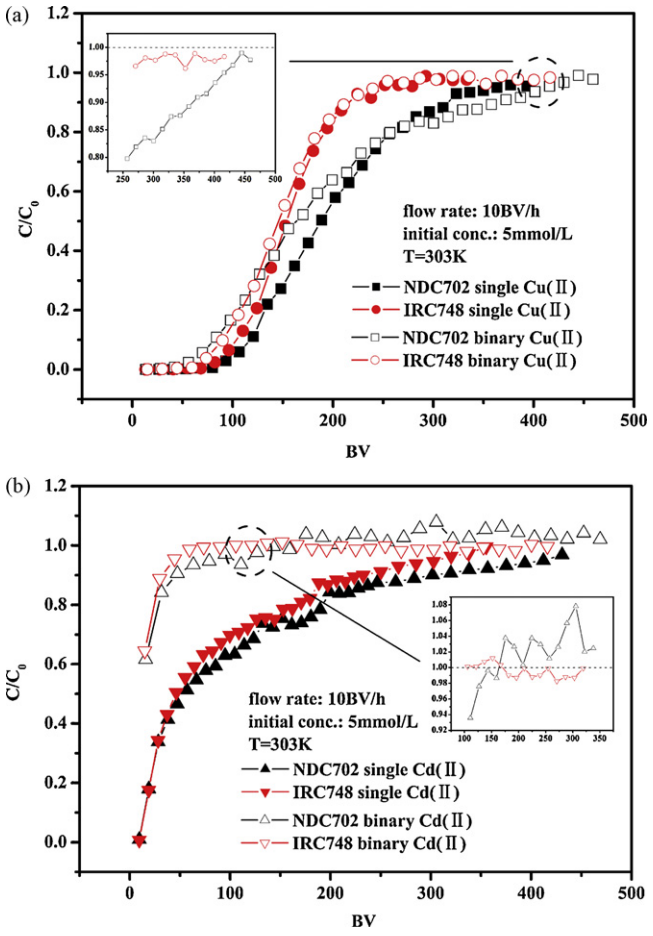

Fig. 7. Breakthrough curves for Cu(II) and Cd(II) adsorption under noncompetitive and competitive conditions at 303 K, pH-value of 5, initial metal ion concentration of 5 mM.

on NDC702 from 1.34 to 0.09 mmol/g is more than IRC748, which is consistent with the tendency of kinetics in binary systems. The reason may exist in the more drastic competition on active site of NDC702. It is probable that cadmium would have been displaced from solid phase by copper as seen from the detail view. However, the feed concentration of cadmium is so much higher than that of displacement, which presents the neglectable change in cadmium concentration. According to HSAB theory, Cd(II) is classified as soft acid which has low affinity with IDA groups, therefore it reduced acutely. In addition, the size of cadmium is greater than copper, which may result in pore blockage. The reduction for NDC702 with a narrow pore size distribution is greater than IRC748 with a broad one. Broadening of the pore size distribution of porous adsorbents can reduce the level of pore blockage, thus reduce the impact on trace metal ion adsorption [40].

3.2.4.2. Column desorption. Elution of Cu(II), Cd(II) in single system are tested by 15 wt% HCl using column technique. More than 97% metal ions are eluted from IRC748, versus around 100% from IRC748, which indicated the sufficient regeneration. The observed similarity in elution behavior could be related to the similar mode of interaction of both resins with metal ions, thus similar functional groups on both IRC748 and NDC702 are further testified.

3.3. Interaction mechanism

As shown in Fig. 8, after adsorption of Pb(II), the pores on the surface of IRC748 turn from orderly porous structure to disordered honeycomb whereas on the section the framework shrink and hence result in some pores and channels. On the other hand, though NDC702 possess less pores on the surface with almost no change on the fovea, similarly, the framework in the slits shrink and show the obvious change on the section. EDX spectra indicate that metal ions can be successfully adsorbed on both outside and inside pores.

Infrared spectra might be useful to speculate the binding forms. Take IRC748 for example, FT-IR spectrum indicates that hydrogen form of both resins exhibit a split carbonyl peak at 1630 and 1730 cm^{-1}. With the copper and lead forms, there is a single broad peak at about 1620 cm^{-1}. This significant change has not been observed in the case of cadmium (Fig. 1). Based on the existing research, the chelation mechanism by iminodiacetate clearly prevails if strong complexes ML are formed, as is the case for copper, while complexation by carboxylate to form $M(HL)_2$ prevails when metal ions with lower complexation constants with the iminodiacetate, such as cadmium. Here, ($-L^{2-}$) coordinates to metal ions using all three donor atoms, like an iminodiacetate in solution (coordination mode I, Scheme 2). As for ($-LH^{-}$), two carboxylates are used for the coordination to metal ions (coordination modeII, Scheme 2) [10,23]. The results for Pb have never allowed to rule out the possibility of formation of weaker 1:2 type metal–ligand associations with the resin groups [33]. According to the decrease of equilibrium pH value, conclusion might be drawn that the adsorption processes of metal ions on IDA-resins could be contributed to both ion exchange and chelation.

Additionally, based on SEM images before and after adsorption, pore size distribution and experimental data above, structures of IRC748 and NDC702 are speculated, as shown in Fig. 9. IRC748 (Fig. 9a) contained more macro/mesopores on the surface with a larger microporosity in the framework of red line, which resulted in a faster rate of adsorption. Lower capacity is resulted from the underutilization of functional groups inside the micropores. Another conjectural structure of IRC748 (Fig. 9b) show that micropores connected external and internal macro/mesopores, which make the mass transfer difficult even impossible to the core of the bead. Combined with SEM images, it is more rational of the former.

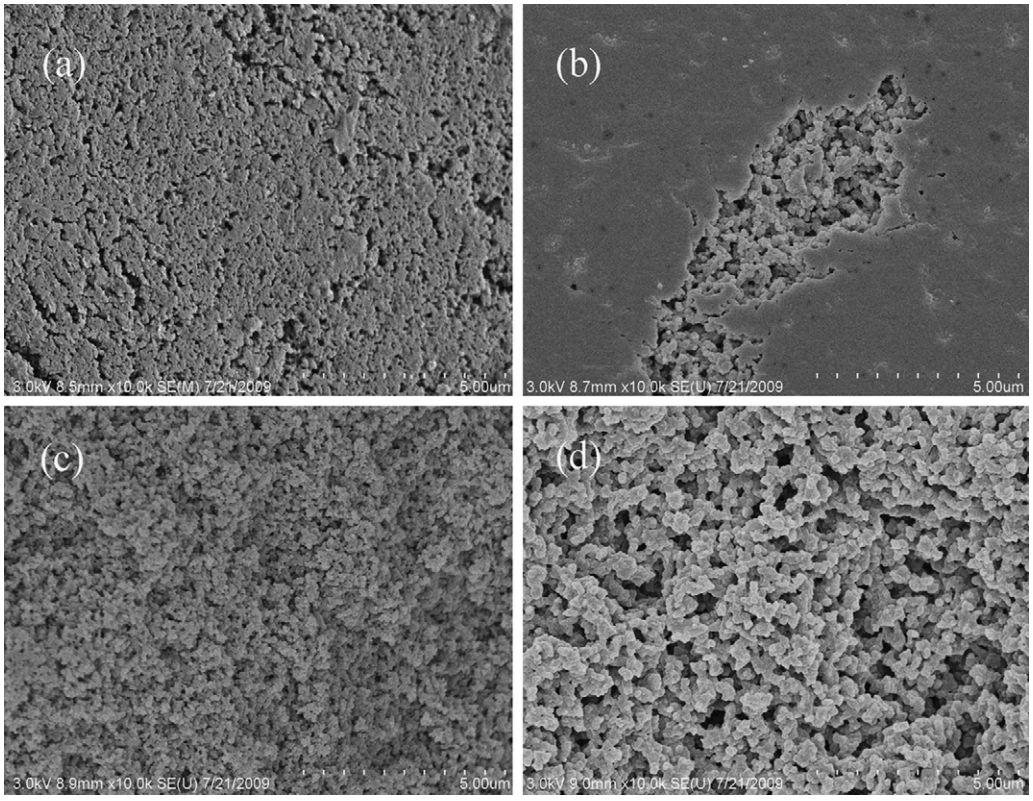

Fig. 8. SEM images of the surface (a and b) and section (c and d) morphologies of IRC748 (a and c) and NDC702 (b and d) after adsorption of Pb(II).

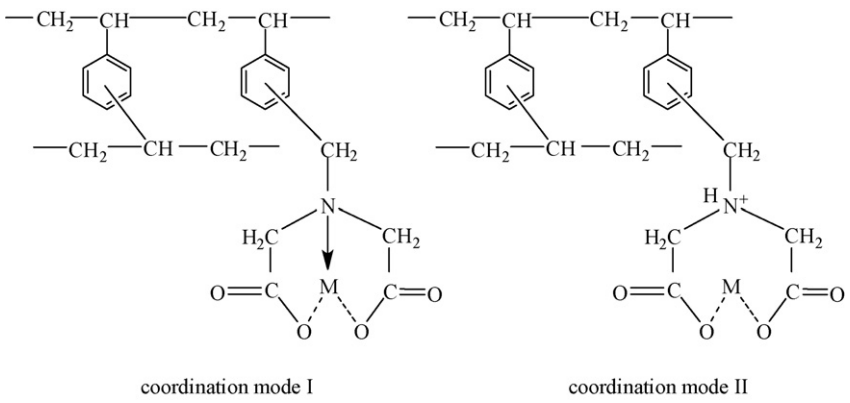

Scheme 2. The interaction configuration of metal ions onto IDA-chelating resins.

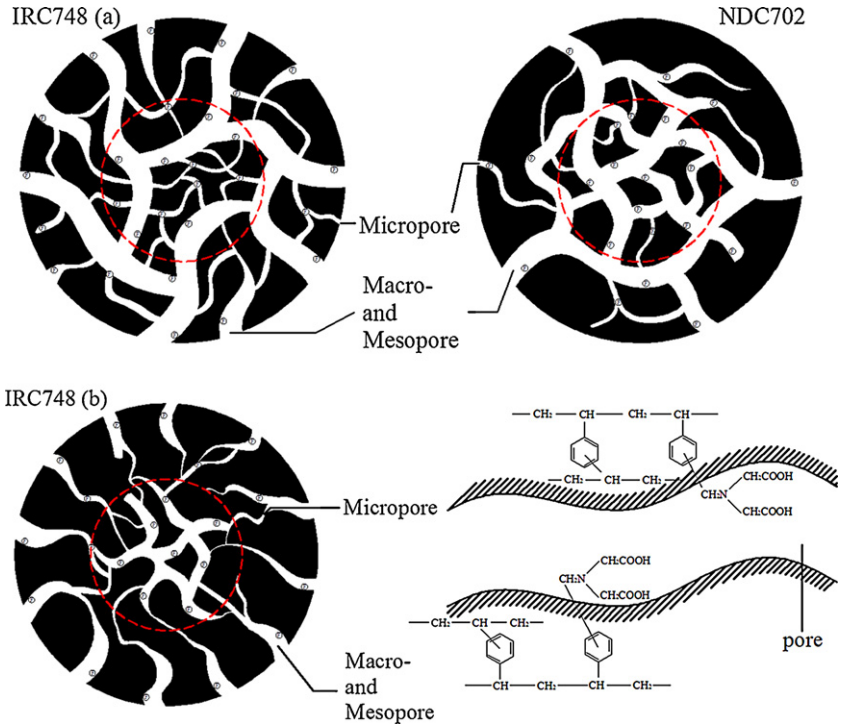

Fig. 9. Schematic illustration for the speculated structures of IRC748 and NDC702.

On the contrary, more macro/mesopores existed in the scale of red line and fewer ones extended to the surface which led to slower rate of adsorption but higher capacity as for NDC702. The distribution of functional groups inside the resin bead (viz. sub-structure) has not been exploited up to now on account of the lack in effective analysis methods. In subsequent researches, the simulation could surely be more accurate by means of several rational experimental design and fine-structure analysis apparatus.

4. Conclusions

The adsorption capacities on IDA-chelating resins IRC748 and NDC702 follow the order of Cu(II) > Pb(II) > Cd(II), due to the complicated impacts of metal ion electronegativity as well as resin pore textures. The equilibrium data agree better with Langmuir isotherm, whose parameters imply the larger capacity of NDC702. The pseudo-second-order model could fit the kinetic curves well, with the greater initial adsorption rate constant of IRC748 for its increasing average pore size and much more outside pores. In binary systems, the high separation factors α of Cu/Cd for IRC748 and NDC702 about 158.1 and 95.6, respectively could be obtained, as a result of which the uptake of Cd(II) decreases sharply. The column desorption efficiency is nearly 100% by 15 wt% HCl, an evidence of very efficient regeneration.

Both ion exchange and chelation are testified to occur during ion adsorption processes. Furthermore, based upon the extreme differences in the above performances, possible sub-structures of IRC748 and NDC702 have been proposed, with more outside macro- and mesopores of the former, versus more inside macro- and mesopores of the latter. Both physical and chemical structures play an important role in ion adsorption onto IDA-chelating resins.

Acknowledgements

The authors are grateful for the financial support of the National Natural Science Foundation of P.R. China (No. 50878103, No. 50938004). They also gratefully thank Modern Analyse Center at Nanjing University and State Key Laboratory of Coordination Chem-

istry for the measurement of EA, FT-IR, SEM and PSD. They also wish to express their appreciations to Prof. HongBin Du and Prof. XiaoZeng You from Coordination Chemistry Institute of Nanjing University for their kind suggestions and help in analyzing the samples and academic composition.

References

[1] W.S.W. Ngah, M.A.K.M. Hanafiah, Bioresour. Technol. 99 (2008) 3935.
[2] K. Kadirvelu, C. Faur-Brasquet, P. Le Cloirec, Langmuir 16 (2000) 8404.
[3] A. Martín-González, S. Díaz, S. Borniquel, A. Gallego, J.C. Gutiérrez, Res. Microbiol. 157 (2006) 108.
[4] B. Danis, P. Wantier, R. Flammang, Ph. Pernet, Y. Chambost-Manciet, G. Coteur, M. Warnau, Ph. Dubois, Sci. Total Environ. 356 (2006) 275.
[5] L.J. Tsai, K.C. Yu, S.T. Ho, J. Hazard. Mater. 148 (2007) 630.
[6] J.M. Sun, C. Shang, J.C. Huang, Environ. Sci. Technol. 37 (2003) 4281.
[7] N. Meunier, P. Drogui, C. Montané, R. Hausler, G. Mercier, J.-F. Blais, J. Hazard. Mater. 137 (2006) 581.
[8] T. Maruyama, H. Matsushita, J. Uchida, F. Kubota, N. Kamiya, M. Goto, Anal. Chem. 76 (2004) 4495.
[9] S.M.C. Ritchie, K.E. Kissick, L.G. Bachas, S.K. Sikdar, C. Parikh, D. Bhattacharyya, Environ. Sci. Technol. 35 (2001) 3252.
[10] A. Yuchi, T. Sato, Y. Morimoto, H. Mizuno, H. Wada, Anal. Chem. 69 (1997) 2941.
[11] Q.R. Zhang, B.C. Pan, B.J. Pan, W.M. Zhang, K. Jia, Q.X. Zhang, Environ. Sci. Technol. 42 (2008) 4140.
[12] M.J. Shaw, P.N. Nesterenko, G.W. Dicinoski, P.R. Haddad, J. Chromatogr. A 997 (2003) 3.
[13] Y.H. Li, J. Ding, Z.K. Luan, Z.C. Di, Y.F. Zhu, C.L. Xu, D.H. Wu, B.Q. Wei, Carbon 41 (2003) 2787.
[14] C. Gao, C.D. Vo, Y.Z. Jin, W.W. Li, S.P. Armes, Macromolecules 38 (2005) 8634.
[15] N.L.D. Filho, D.R. Carmo, Talanta 68 (2006) 919.
[16] J.S. Li, X.Y. Miao, Y.X. Hao, J.Y. Zhao, X.Y. Sun, L.J. Wang, J. Colloid Interf. Sci. 318 (2008) 309.
[17] A. Sayari, S. Hamoudi, Y. Yang, Chem. Mater. 17 (2005) 212.
[18] J.P. Chen, S.N. Wu, Langmuir 20 (2004) 2233.
[19] S.R. Kanel, B. Manning, L. Charlet, H. Choi, Environ. Sci. Technol. 39 (2005) 1291.
[20] H. Gen-Fuhrman, J.C. Tjell, D. McConchie, Environ. Sci. Technol. 38 (2004) 2428.
[21] S. Pramanik, P.K. Dhara, P. Chattopadhyay, Talanta 63 (2004) 485.
[22] J.L. Stair, J.A. Holcombe, Anal. Chem. 79 (2007) 1999.
[23] M. Pesavento, R. Biesuz, M. Gallorini, A. Profumo, Anal. Chem. 65 (1993) 2522.
[24] D. Muraviev, A. Gonzalo, M. Valiente, Anal. Chem. 67 (1995) 3028.
[25] D. Atzei, T. Ferri, C. Sadun, P. Sangiorgio, R. Caminiti, J. Am. Chem. Soc. 123 (2001) 2552.
[26] K.A. Mumford, K.A. Northcott, D.C. Shallcross, G.W. Stevens, I. Snape, Ind. Eng. Chem. Res. 46 (2007) 3766.
[27] Q.L. Lu, G.A. Sorial, Chemosphere 55 (2004) 671.
[28] F.N. Xi, J.M. Wu, X.F. lin, J. Chromatogr. A 1125 (2006) 38.
[29] M. Choi, J. Jang, J. Colloid Interf. Sci. 325 (2008) 287.
[30] K. Zhang, W.H. Cheung, M. Valix, Chemosphere 60 (2005) 1129.
[31] K.C. Kang, S.S. Kim, J.W. Choi, S.H. Kwon, J. Ind. Eng. Chem. 14 (2008) 131.
[32] S.L. Sun, A.Q. Wang, J. Hazard. Mater. 131 (2006) 103.
[33] M.E. Malla, M.B. Alvarez, D.A. Batistoni, Talanta 57 (2002) 277.
[34] B.L. Rivas, A.E. Maureira, M.A. Mondaca, Eur. Polym. J. 44 (2008) 2330.
[35] M. Kruk, M. Jaroniec, Chem. Mater. 13 (2001) 3169.
[36] A. Baraka, P.J. Hall, M.J. Heslop, React. Funct. Polym. 67 (2007) 585.
[37] C.K. Liu, R.B. Bai, L. Hong, J. Colloid Interf. Sci. 303 (2006) 99.
[38] D.K. Kweon, J.K. Choi, E.K. Kim, S.T. Lim, Carbohydr. Polym. 46 (2001) 171.
[39] C.A. Christophi, L. Axe, J. Environ. Eng. 126 (2000) 66.
[40] C. Pelekani, V.L. Snoeyink, Water Res. 33 (1999) 1209.
[41] S.Y. Kang, J.U. Lee, S.H. Moon, K.W. Kim, Chemosphere 56 (2004) 141.